ELSEVIER

Coordination Chemistry Reviews
190–192 (1999) 471–491

COORDINATION CHEMISTRY REVIEWS

www.elsevier.com/locate/ccr

Cooperative phenomena and light-induced bistability in iron(II) spin-crossover compounds

Andreas Hauser [a,*], Jelena Jeftić [b], Harald Romstedt [b], Roland Hinek [c], Hartmut Spiering [c]

[a] *Département de chimie physique, Université de Genève, 30 quai Ernest-Ansermet, CH-1211 Geneva 4, Switzerland*

[b] *Departement für Chemie und Biochemie, Universität Bern, Freiestrasse 3, CH-3000 Bern 9, Switzerland*

[c] *Institut für Anorganische Chemie, Johannes-Gutenberg Universität, Staudingerweg 9, D-55099 Mainz, Germany*

Accepted 13 March 1999

Contents

Abstract

In iron(II) spin-crossover compounds, the transition from the $^1A_1$ low-spin state at low temperatures to the $^5T_2$ high-spin state at elevated temperatures is accompanied by a large increase in metal-ligand bond lengths. The resulting elastic interactions may be pictured as an internal pressure which is proportional to the concentration of the low-spin species.

* Corresponding author. Tel.: +41-22-7026559; fax: +41-22-7026103.
E-mail address: andreas.hauser@chiphy.unige.ch (A. Hauser)

0010-8545/99/$ - see front matter
PII: S0010-8545(99)00111-3

Because pressure stabilises the low-spin state relative to the high-spin state this results in a positive feedback. Thermal transition curves in neat iron(II) spin-crossover compounds are thus invariable much steeper than in diluted mixed crystals, and the high-spin → low-spin relaxation following the light-induced population of the high-spin state at low temperatures is self-accelerating. Strong interactions give rise to a thermal hysteresis, and light-induced bistabilities may be observed for compounds with initially a high-spin ground state and the potential for a light-induced population of the low-spin state. For such compounds, the increasing internal pressure may stabilise the low-spin state sufficiently so that it becomes the molecular ground state above some critical light-induced low-spin fraction. Secondary effects of the elastic interactions include crystallographic phase transitions, inhomogeneous distributions of sites, and anomalies such as steps in the transition curve.

Keywords: Iron(II) coordination compounds; Spin-crossover; Cooperative effects; High-spin → low-spin relaxation; Bistability

1. Introduction

Of all octahedrally coordinated transition metal complexes with electronic configurations from d^4 to d^7 exhibiting the phenomenon of a thermal spin transition, those of d^6 iron(II) are by far the most studied [1]. This is due to the fact, that for these, the entropy driven, thermal spin transition from the $^1A_1(t_{2g}^6)$ low-spin (LS) state, populated at low temperatures, to the $^5T_2(t_{2g}^4e_g^2)$ high-spin (HS) state, populated at elevated temperatures, shows a large variety in its behaviour. Transition curves, that is, the fraction of complexes in the HS state γ_{HS} versus temperature, for diluted systems, such as spin-crossover complexes in solution or in diluted mixed crystals, are gradual, following the prediction of a Boltzmann distribution between the two vibronic manifolds. In neat spin-crossover compounds, however, cooperative interactions of elastic origin due to the large differences in metal-ligand bond lengths $\Delta r_{HL} = r_{HS} - r_{LS}$ of ~ 0.16–0.21 Å [2] and the concomitant differences in crystal volumes $\Delta V_{HL} = V_{HS} - V_{LS}$ of ~ 20–30 Å^3 per molecular unit [3] between the two states, result in generally much steeper transition curves [4], hysteresis behaviour with [5] and without accompanying crystallographic phase transition [6], stepwise [7] and partial transitions [8]. Likewise, cooperative effects influence the HS → LS relaxation. Whereas in diluted systems, the HS → LS relaxation following the light-induced population of the HS state at low temperatures as a metastable state [9] is single exponential, the relaxation curves in neat iron(II) spin-crossover compounds show a strongly self-accelerating behaviour [10].

In early discussions of cooperative effects in iron(II) spin-crossover compounds, the interaction was regarded as nearest-neighbour interaction [11]. It was, however, treated in mean-field approximation, resulting in an effective long-range interaction. Based on elasticity theory, Spiering et al. [4] justified the mean-field approach physically by showing that elastic interactions, in fact, give rise to truly long-range contributions, and that these may be pictured as an internal pressure which increases linearly with the concentration of the LS species. In Section 2 we give a

brief overview of the thermodynamics of this model, including the application of an external pressure and its consequences for the HS → LS relaxation, together with a case study of a system for which all observations can be consistently described within the mean-field approach, namely $[Fe(ptz)_6](BF_4)_2$ (ptz = 1-propyltetrazole).

Not all neat systems follow the predictions of the first order approach. In particular, steps in the transition curve for compounds for which all complexes are crystallographically equivalent cannot be explained on this basis. Such steps are thought to be due to additional specific nearest neighbour interactions favouring the formation of chess board like HS–LS patterns over a limited temperature range. This point and its consequences for the HS → LS relaxation in the compound $[Fe(pic)_3]Cl_2 \cdot EtOH$ (pic = picolylamine) are discussed in Section 3.

It is well known that even in the crystalline state electronic energies of excited states of transition metal ions are inhomogeneously distributed [12]. Particularly in iron(II) spin-crossover compounds with crystallographic disorder phenomena, such an inhomogeneous distribution may easily be on the order of magnitude of the zero-point energy difference ΔE°_{HL} itself. In Section 4, the effects of an inhomogeneous distribution on both the thermal spin transition as well as the HS → LS relaxation are discussed.

A thermal hysteresis is the manifestation of a macroscopic bistability. Such bistabilities are essential for applications of spin-crossover compounds in data storage devices [13]. In Section 5 light-induced bistabilities are presented. These are particularly important with a view towards fully optical devices.

2. The first order approximation

2.1. The thermal spin transition

For a system of non-interacting complexes, for instance in a mixed crystal with the spin-crossover complexes doped into an inert host lattice with a mole fraction $x \to 0$, the thermal LS ⇄ HS equilibrium is described by:

$$\Delta G_{HL} = \Delta H^{x \to 0}_{HL} - T\Delta S^{x \to 0}_{HL} = -k_B T \ln\left(\frac{\gamma_{HS}}{1-\gamma_{HS}}\right) \quad (1)$$

where $\Delta H^{x \to 0}_{HL}$ and $\Delta S^{x \to 0}_{HL}$ are the differences in enthalpy and entropy between the HS and the LS vibronic manifolds at infinite dilution. In principle, the two quantities are temperature dependant as ΔG_{HL} for $T < 100$ K deviates from a linear temperature dependence [14], but in the actual evaluation of experimental data their temperature dependence across the thermal transition is often regarded as negligible. The large positive entropy due to the fifteen-fold electronic degeneracy of the HS state of iron(II) and the higher density of vibrational states drives the spin transition gradually but almost quantitatively from the LS state at low temperatures to the HS state at elevated temperatures. The transition temperature, defined as the temperature at which $\gamma_{HS} = 0.5$, is given by $T_{1/2} = \Delta H^{x \to 0}_{HL} / \Delta S^{x \to 0}_{HL}$.

For a concentrated spin-crossover system an interaction term has to be added to Eq. (1). In the mean-field approach [11], which assumes a random distribution of HS and LS complexes at all times, this interaction term is developed in a power series according to

$$\Delta G_{HL} = \Delta H_{HL}^{x\to 0} - T\Delta S_{HL}^{x\to 0} + D - 2G\gamma_{HS} \tag{2}$$

where the energy shift Δ accounts for the difference in interaction of the two states with the reference lattice, and therefore depends upon the reference lattice for which $\Delta H_{HL}^{x\to 0}$ was determined. Γ is the actual interaction constant which accounts for the interaction between spin-changing complexes. Spiering et al. [4,15] showed that Δ and Γ can be related to the elastic properties of the lattice. In their continuum model the interaction is inherently treated as of a long-range nature, and Γ has to be positive. It may thus be regarded as an internal pressure which increases in proportion to the LS fraction $\gamma_{LS} = 1 - \gamma_{HS}$. Because pressure destabilises the HS state with respect to the LS state, this results in a positive feedback and thus explains the generally steeper transition curves for neat compounds as compared to diluted systems.

For a reference lattice which is similar to the LS lattice of the neat spin-crossover compound, $\Delta = 0$. For one which is similar to the HS lattice, as for instance with zinc(II) as the inert metal ion, $\Delta = 2\Gamma$. Fig. 1(a) shows transition curves calculated according to Eq. (2) for a series of values of the interaction parameter Γ, with $\Delta = 2\Gamma$, and using typical values for $\Delta H_{HL}^{x\to 0}$ and $\Delta S_{HL}^{x\to 0}$ of 500 cm^{-1} and 5 cm^{-1} K^{-1}, respectively. For increasing values of Γ, the transition curves become successively steeper, and they shift to higher temperatures according to $T_{1/2} = (\Delta H_{HL}^{x\to 0} + \Delta - \Gamma)/\Delta S_{HL}^{x\to 0}$. Above a critical value of $\Gamma_c \approx 190$ cm^{-1}, the interaction results in hysteresis behaviour.

Fig. 1(b) shows the experimental results for the spin-crossover complex $[Fe(ptz)_6]^{2+}$ as neat $[Fe(ptz)_6](BF_4)_2$ and doped into the isostructural $[Zn(ptz)_6](BF_4)_2$ [16,17]. The spin transition for the diluted compound is gradual with $T_{1/2} = 95$ K, the one for the neat compound is steep and shows a thermal hysteresis. However, this hysteresis is not due to the interaction as such. Rather it is due to a crystallographic phase transition with $T_c^{\downarrow} = 128$ K and $T_c^{\uparrow} = 135$ K [5], which accompanies the spin transition. By rapidly cooling the sample, the crystallographic high-temperature phase can be super-cooled down to cryogenic temperatures. The spin transition in this super-cooled phase is still complete and steep with $T_{1/2} = 125$ K, but without hysteresis. A least squares fit of Eq. (1) to the data of the diluted system results in values for $\Delta H_{HL}^{x\to 0}$ and $\Delta S_{HL}^{x\to 0}$ of 462(6) cm^{-1} and 4.9(1) cm^{-1} K^{-1}, respectively. These values have to be regarded as $\Delta H_{HL}^{x\to 0}$ and $\Delta S_{HL}^{x\to 0}$ at $T_{1/2}$. Using them as fixed values in a least squares fit of Eq. (2) to the transition curve of the neat iron(II) compound in its high-temperature phase gives values for Δ and Γ of 310(8) and 165(8) cm^{-1}, respectively. Even though these values were obtained neglecting the temperature dependence of $\Delta H_{HL}^{x\to 0}$ and $\Delta S_{HL}^{x\to 0}$, they are reasonably close to values obtained using more sophisticated procedures [16,17]. The ratio $\Delta/\Gamma \approx 2$, predicted for the isostructural zinc lattice, is nicely fulfilled.

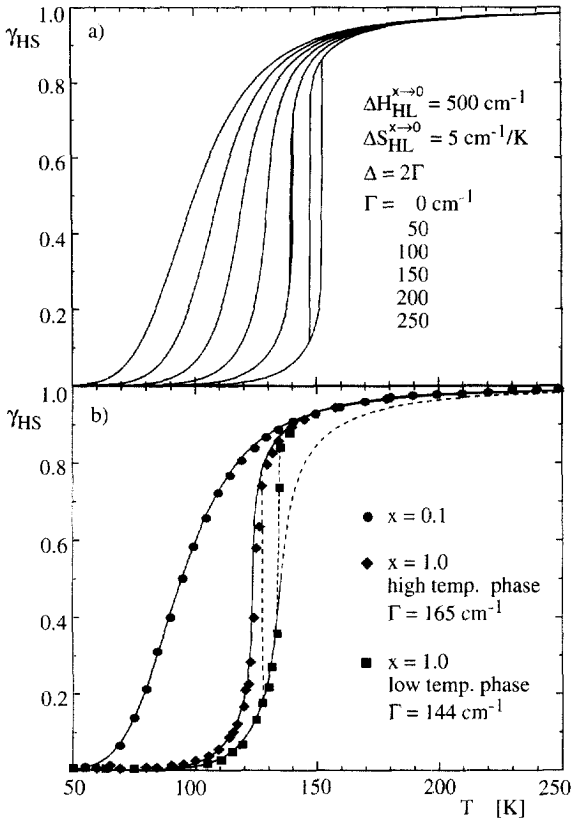

Fig. 1. (a) Calculated spin transition curves according to Eq. (2) with $\Delta H_{HL}^{x\to 0}$ = 500 cm^{-1}, $\Delta S_{HL}^{x\to 0}$ = 5 cm^{-1} K^{-1}, Γ between 0 and 250 cm^{-1} and $\Delta = 2\Gamma$. (b) Thermal transition curves for (●) $[Zn_{1-x}Fe_x(ptz)_6](BF_4)_2$ (x = 0.1) and (◆, ■) $[Fe(ptz)_6](BF_4)_2$. (—) Curves calculated with $\Delta H_{HL}^{x\to 0}$ = 462 cm^{-1}, $\Delta S_{HL}^{x\to 0}$ = 4.9 cm^{-1} K^{-1}, and $\Delta = \Gamma = 0$ for the diluted system, and Δ = 310 and 380 cm^{-1}, and Γ = 165 and 144 cm^{-1} for the neat compound in the high-temperature and the low-temperature phase, respectively (adapted from Refs. [16,17]).

The above mean-field model has, in fact, been very successful in treating a wealth of experimental data. In a series of papers Spiering et al. [4,14] showed that for mixed crystals of general composition $[M_{1-x}Fe_x(pic)_3]X_2$·solv (solv = MeOH, EtOH; X = Cl, Br; M = Co, Zn, Mn) the interaction constant scales with x, and Martin et al. [6] presented data for the mixed crystal series $[M_{1-x}Fe_x(btr)_2(NCS)_2]$·$2H_2O$ (btr = 4,4′-bis-1,2,4-triazole, M = Co, Ni), for which the interaction constant Γ of 400 cm^{-1} is large enough to result in a hysteresis for $x > 0.4$. Furthermore, for the nickel host the ratio $\Delta/\Gamma \approx 1$, as expected for a host lattice with a metal ion having an ionic radius half way in between iron(II) HS and LS.

2.2. The HS→LS relaxation

In diluted mixed crystals, the HS→LS relaxation following the light-induced population of the HS state as metastable state via ligand-field and MLCT excited states [9,18] is single exponential. It is basically a non-adiabatic multi-phonon process [19], and the relaxation rate constant is given by [20]

$$k_{HL}(T) = \frac{2\pi}{\hbar^2\omega}\beta_{HL}^2 F_n(T) \tag{3}$$

β_{HL} is the electronic coupling matrix element provided by second order spin-orbit coupling and has a value of $\sim 150\ cm^{-1}$ [20]. $\hbar\omega$ is the vibrational frequency of the accepting mode, which in this case is the metal–ligand breathing mode with typical frequencies of $\sim 250\ cm^{-1}$ and a corresponding force constant f of 2×10^5 dyn cm^{-1}. $F_n(T)$ is the thermally averaged Franck–Condon factor given by:

$$F_n(T) = \frac{\sum |\langle \chi_{m'}|\chi_m\rangle|^2 e^{-\hbar\omega m/k_B T}}{\sum e^{-\hbar\omega m/k_B T}} \tag{4}$$

The sum goes over all vibrational levels of the HS state m, and the individual Franck–Condon factors have to be evaluated for $m' = m + n$, with the reduced energy gap $n = \Delta E^{\circ}_{HL}/\hbar\omega$, in order to ensure energy conservation. For a diluted system, the zero-point energy difference $\Delta E^{\circ}_{HL} = \Delta H^{x\to 0}_{HL}(T\to 0)$. It is typically somewhat smaller than $\Delta H^{x\to 0}_{HL}$ at $T_{1/2}$ as obtained from the thermal transition curve [14].

At $T\to 0$ the $F_n(T)$ factor takes the simple form:

$$F_n(T\to 0) = |\langle \chi_n|\chi_o\rangle|^2 = \frac{e^{-S}S^n}{n!} \tag{5}$$

with the reorganisation energy in units of $\hbar\omega$ given by the Huang–Rhys factor $S = 1/2f\Delta Q^2/E\omega$. With the above mentioned values and $\Delta Q_{HL} = \sqrt{6}\Delta r_{HL} \approx 0.5$ Å, a value for S of ~ 45 has been estimated [21].

In the limit of strong vibronic coupling ($S \gg n$), the theory of non-adiabatic multi-phonon relaxation predicts (a) a temperature independent HS→LS relaxation below ~ 50 K, corresponding to a nuclear tunnelling process from the lowest vibrational level of the HS state governed by Eq. (5), and (b) a thermally activated process at elevated temperatures, to be regarded as tunnelling from thermally populated vibrational levels of the HS state [19]. This behaviour has been verified experimentally [21,22]. The important point to note is, that as in the strong vibronic coupling limit $|\langle \chi_n | \chi_o\rangle|^2$ is an almost exponential function of n, the low-temperature tunnelling rate constant $k_{HL}(T\to 0)$, too, depends almost exponentially on n and therefore on ΔE°_{HL}. Experimental values for $k_{HL}(T\to 0)$, in fact, range from $10^{-6}\ s^{-1}$ for spin-crossover systems with $T_{1/2} \leq 100$ K and thus values of $n \leq 1$, to $10^{6}\ s^{-1}$ for low-spin systems with $n \geq 10$ [21].

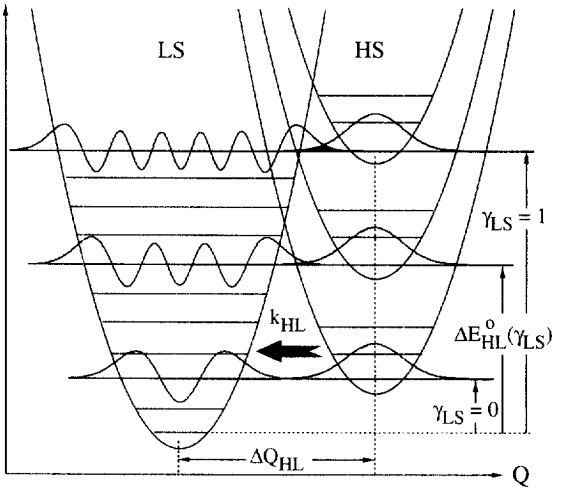

Fig. 2. Schematic representation of HS and LS potential wells along the reaction coordinate Q. The zero-point energy difference ΔE°_{HL} depends primarily on ligand characteristics. In concentrated spin-crossover compounds it is strongly influenced by cooperative effects. In the mean-field approximation, ΔE°_{HL} is regarded as a linear function of the LS fraction.

As shown schematically in Fig. 2, the exponential dependence of k_{HL} $(T \rightarrow 0)$ on ΔE°_{HL} has important consequences for the HS $\rightarrow$ LS relaxation in neat iron(II) spin-crossover compounds, because ΔE°_{HL} now increases as a function of the LS fraction γ_{LS} according to:

$$\Delta E^{\circ}_{HL}(\gamma_{LS}) = \Delta E^{\circ}_{HL}(\gamma_{LS} = 0) + 2G\gamma_{LS} \tag{6}$$

This results in a self-accelerating rate constant for the HS $\rightarrow$ LS relaxation of the general form

$$k_{HL}(T, \gamma_{LS}) = k^{\circ}_{HL}(T)\ e^{\alpha(T)\gamma_{LS}} \tag{7}$$

The rate constant at the beginning of the relaxation, $k^{\circ}_{HL}(T)$, is given by Eqs. (3)–(5), with the initial reduced energy gap $n_o = \Delta E^{\circ}_{HL}(\gamma_{LS} = 0)/E\omega$. At low temperatures and for values of $n_o \leq 1$, the acceleration factor $\alpha(T \rightarrow 0) \approx \ln(S)2\Gamma/\hbar\omega$. For larger values $\alpha(T \rightarrow 0)$ decreases according to $\alpha(T \rightarrow 0) \approx \ln(S/n_o)2\Gamma/\hbar\omega$. Likewise, for higher temperatures the analytical form of Eq. (7) is still valid, but α becomes proportional to $1/T$. Fig. 3 shows the acceleration factor α as a function of temperature with n_o as parameter calculated using Eqs. (3)–(7) together with a value for Γ of 165 cm^{-1} and the above standard values for S and $\hbar\omega$.

Fig. 4 shows a series of HS $\rightarrow$ LS relaxation curves for $[Fe(ptz)_6](BF_4)_2$ in the super-cooled high-temperature phase following a quantitative light-induced population of the HS state between 50 and 60 K [10,17]. The self-accelerating rate constant of Eq. (7) results in an excellent fit to the experimental data. In Fig. 3 the experimental values of α for $[Fe(ptz)_6](BF_4)_2$ between 40 and 70 K are included. The agreement with the theoretical prediction is very good. In particular, the experimen-

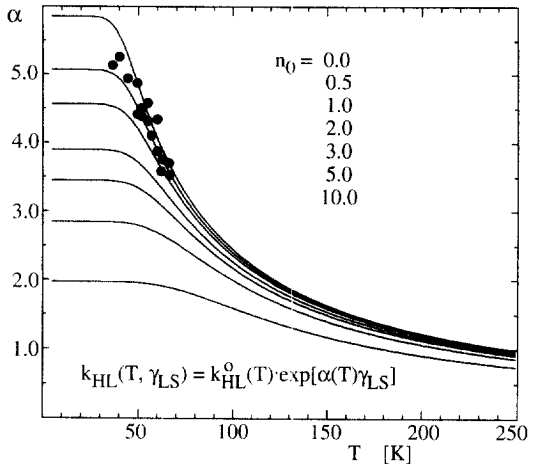

Fig. 3. Self-acceleration factor α for the HS → LS relaxation in concentrated spin-crossover compounds as a function of temperature. (●) Experimental values for $[Fe(ptz)_6](BF_4)_2$, calculated according to Eqs. (3)–(6) with $S = 45$, $\hbar\omega = 250\ cm^{-1}$, $\Gamma = 165\ cm^{-1}$, and various values for the initial reduced energy gap $n_0 = \Delta E^{\circ}_{HL}(\gamma_{LS} = 0)/\hbar\omega$.

tal value of ~ 5 for the lowest temperature measured is close to the limiting value of 5.1 calculated with $n_o = 0.5$.

The key message of this and the preceding section is, that for $[Fe(ptz)_6](BF_4)_2$ in the crystallographic high-temperature phase with its close to octahedral symmetry, the straightforward mean-field approach to cooperative effects consistently describes the thermal spin transition and the HS → LS relaxation.

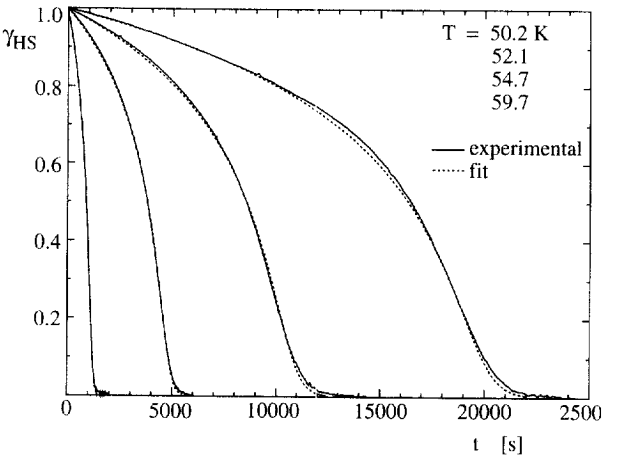

Fig. 4. HS → LS relaxation curves for $[Fe(ptz)_6](BF_4)_2$ in the supercooled high-temperature phase between 50 and 60 K following a quantitative light-induced population of the HS state. (——) Experimental, (---) least-squares fit according to Eq. (7) (adapted from Ref. [10]).

2.3. External pressure

The picture of cooperative effects as a changing internal pressure can be given some physical meaning by comparison with the effects of external pressure, p, upon the thermal spin transition and the relaxation kinetics. With an external pressure p a work term of the form $p\Delta V_{HL}$ has to be added to Eq. (2) according to:

$$\Delta G_{HL} = \Delta H_{HL}^{x\to 0} - T\Delta S_{HL}^{x\to 0} + \Delta - 2G\gamma_{HS} + p\Delta V_{HL} \quad (8)$$

On a microscopic scale, external pressure increases the zero-point energy difference ΔE_{HL}° between the HS and the LS state and thus increases the Franck–Condon factor for the horizontal transition. For small external pressures, that is in the limit of a linear increase of ΔE_{HL}° with pressure, an equation similar to Eq. (7) holds for the HS → LS relaxation rate constant:

$$k_{HL}(T,p) = k_{HL}^{\circ}(T)e^{\beta(T)p} \quad (9)$$

where the self-acceleration factor α has been replaced by a temperature dependent pressure coefficient β. In the low-temperature tunnelling region and for $n_o \leq 1$, this pressure coefficient $\beta(T\to 0) \approx \ln(S)\Delta V_{HL}/\hbar\omega$. For larger values of the reduced energy gap it becomes a function of n_o according to $\beta(T\to 0) \approx \ln(S/n_o)\Delta V_{HL}/\hbar\omega$, and in the thermally activated region it takes the form of the classical activation formula $\beta(T) = -\Delta V_{HL}^{\dagger}/k_B T$, where $\Delta V_{HL}^{\dagger}$ is the activation volume [23].

Fig. 5(a) shows thermal transition curves for $[Zn_{1-x}Fe_x(ptz)_6](BF_4)_2$ ($x = 0.1$) at ambient pressure and at external pressures up to 1 kbar determined from low to high temperatures. As expected for a large positive value of ΔV_{HL}, external pressure shifts the spin transition to higher temperatures. A value for ΔV_{HL} of 26 Å^3/complex can be derived from these curves using Eq. (8). Pressures above 300 bar induce a crystallographic phase transition even in the diluted compound [17]. Transition curves of the neat PF_6-derivative $[Fe(ptz)_6](PF_6)_2$ at 1 bar, 500 bar and 1 kbar are shown in Fig. 5(b). For ΔV_{HL} a value of 28 Å^3/complex [24] can be derived from these curves, following the procedure described by Adler et al. [25]. Values on the same order have been found for a number of iron(II) spin-crossover complexes [3].

In $[Zn_{1-x}Fe_x(ptz)_6](BF_4)_2$ ($x = 0.1$) relaxation curves following the light-induced population of the HS state remain single exponential. But, as predicted, for pressures up to 1 kbar the relaxation rate constants increase exponentially with pressure. Fig. 6 shows the experimentally determined pressure coefficients β versus $1/T$ for $[Zn_{1-x}Fe_x(ptz)_6](BF_4)_2$ ($x = 0.1$) in both crystallographic phases. The experimental low-temperature value for $\beta(T\to 0)$ of ~ 2.7 kbar^{-1} corresponds to an increase of the low-temperature tunnelling rate constant of one order of magnitude per kbar. It is somewhat larger than the value of 2.2 kbar^{-1} predicted for $\Delta V_{HL} \approx 26$ Å^3/complex and the standard values for S and $\hbar\omega$ of 45 and 250 cm^{-1}, respectively. This is thought to be due to a small reduction in the value of Δr_{HL} under external pressure as a result of the smaller force constant for the HS as compared to the one of the LS state. From the thermally activated region a value for the activation volume $\Delta V_{HL}^{\dagger}$ of -17 Å^3/complex can be derived. This puts the transition state right in between the HS and the LS state along the reaction coordinate.

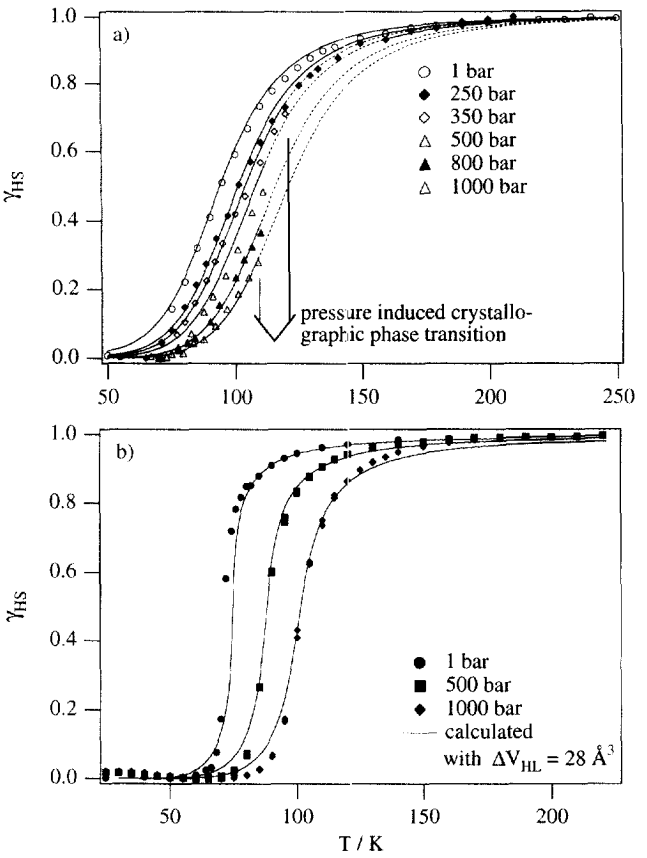

Fig. 5. (a) Thermal transition curves of $[Zn_{1-x}Fe_x(ptz)_6](BF_4)_2$ ($x = 0.1$) at ambient pressure and for pressures up to 1 kbar. Samples were cooled to 15 K before applying pressure, transition curves were recorded in the heating mode. Symbols: experimental. Full lines: calculated with $\Delta V_{HL} = 26$ Å^3. (b) Thermal transition curves for $[Fe(ptz)_6](PF_6)_2$ at 1 bar, 500 bar and 1 kbar. Full lines: calculated with $\Delta V_{HL} = 28$ Å^3 (adapted from Refs. [17,24]).

It may be concluded that on a microscopic scale cooperative effects have much the same influence on the spin-crossover complexes as an external pressure. For $[Fe(ptz)_6](BF_4)_2$ in the high-temperature phase, for example, an external pressure of ~ 2 kbar would be required in order to accelerate the HS → LS relaxation by the same amount as the cooperative effects accelerate it from start to end of the HS → LS relaxation.

3. Specific nearest neighbour interactions

As demonstrated above, the mean-field approach which treats all interactions as of long-range origin can consistently describe a large body of experimental results.

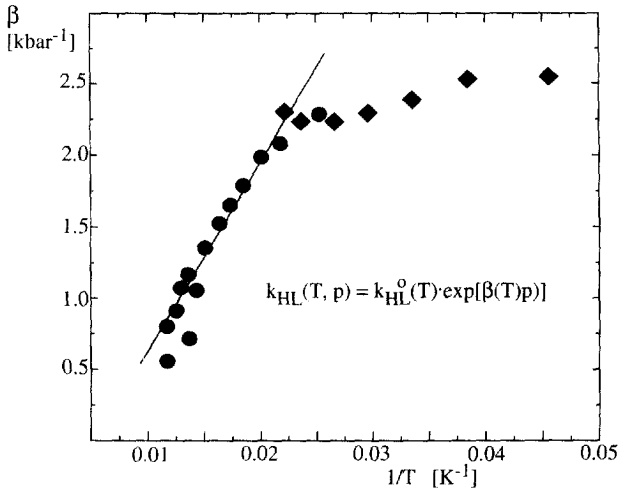

Fig. 6. Acceleration factor β for the acceleration of the HS→LS relaxation under external pressure for $[Zn_{1-x}Fe_x(ptz)_6](BF_4)_2$ ($x = 0.1$) in the normal phase (●) and in the pressure induced phase (◆). From the linear behaviour at elevated temperatures the volume of activation $\Delta V^{\neq}_{HL} = -17$ Å^3.

However, it fails in a few but very important cases. For instance, it cannot account for the step in the transition curve of $[Fe(pic)_3]Cl_2\cdot EtOH$ [7] (see Fig. 7), in which all complexes are crystallographically equivalent. This phenomenon requires that, in addition to the long-range pressure type interactions, specific nearest-neighbour interactions have to be considered. Overall, the transition curve of $[Fe(pic)_3]Cl_2\cdot EtOH$ is very steep. This indicates that the dominant long-range interaction favouring the majority species is large, with a value for the interaction constant Γ close to the critical value above which a hysteresis is to be expected.

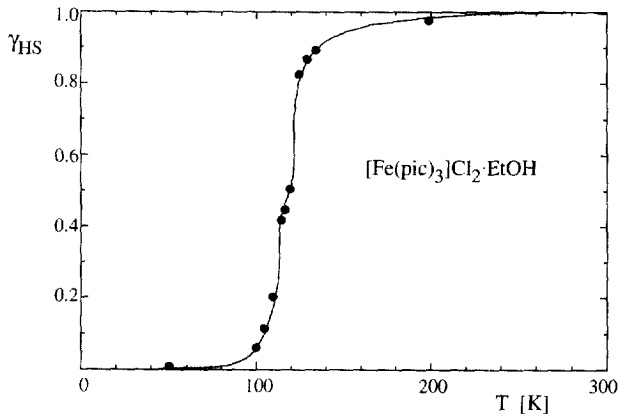

Fig. 7. Thermal spin transition curve for $[Fe(pic)_3]CL_2\cdot EtOH$. (●) From optical spectra; (—) from magnetic susceptibility (adapted from Ref. [29]).

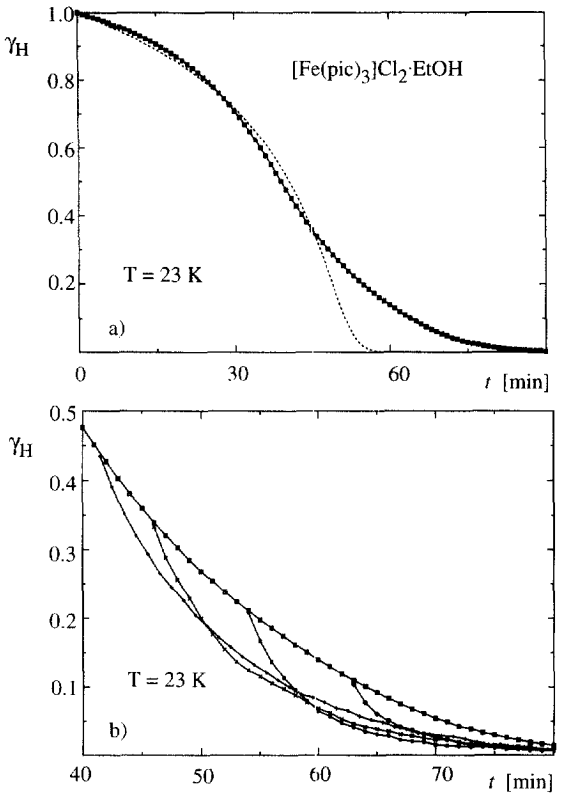

Fig. 8. HS → LS relaxation curves for [Fe(pic)$_3$]CL$_2$·EtOH at 23 K. (a) Full curve (□) experimental; (---) mean-field prediction. (b) Relaxation curves following a partial population of the HS state with the full curve as reference curve (adapted from Ref. [29]).

However, specific nearest-neighbour interactions stabilise HS–LS pairs within the temperature interval of the step, resulting in a non-random distribution of HS and LS molecules in the form of chess board like patterns [26].

Bouseksou et al. [27] proposed an Ising-like model for treating nearest-neighbour interactions. In the mean-field approximation this results in the same algebraic equation as the elastic continuum model of Spiering et al. [4], only the physical interpretation of the parameters is very different. However, Monte Carlo methods as proposed by Linares et al. [28] allow an exact solution of the Ising-like Hamiltonian. Kohlhaas et al. [26] applied the method successfully to the spin transition for the mixed crystal series [$Zn_{1-x}Fe_x$(pic)$_3$]Cl$_2$·EtOH. In their approach they included a long-range part to the interaction modelled along the lines described in Section 2 as well as a short-range contribution modelled with the above mentioned Ising-like Hamiltonian for nearest and next nearest neighbour interactions.

Nearest neighbour interactions will also lead to a build-up of correlations during the HS → LS relaxation following the light-induced population of the HS state as

metastable state at low temperatures [29]. Thus, deviations from the comparatively simple, exponential self-accelerating behaviour of Section 2 are expected. Fig. 8(a) shows the full HS → LS relaxation curve for $[Fe(pic)_3]Cl_2 \cdot EtOH$ at 23 K. Initially it is self-accelerating, but for $\gamma_{HS} < 0.5$ it slows down again when compared to the extrapolation of the initial acceleration according to the mean-field approach. Fig. 8(b) shows relaxation curves obtained after a partial light-induced population of the HS state, using the irradiation technique described in Ref. [29] in order to minimise concentration gradients. The partial curves are displaced along the time axis in such a way that the initial HS fractions are equal to the value of the full curve, which is included as reference curve in Fig. 8(b). Obviously they do not coincide with the full curve. The key difference between the full curve and the partial curves is that for the former, at a given value of γ_{HS}, correlations have been allowed to build up, whereas for the same value of γ_{HS} obtained through partial population by irradiation, HS and LS complexes are distributed randomly. Naturally, the relaxation rates at this value of γ_{HS} differ for the two cases. The relaxation behaviour for $[Fe(pic)_3]Cl_2 \cdot EtOH$, both for the full curve as well as for the partial curves [29], can be modelled in a dynamic Monte Carlo simulation based on the same combination of long-range and Ising-like short-range interaction terms proposed by Kohlhaas et al. [26] for the thermal spin transition.

4. Inhomogeneous distributions

As mentioned in Section 2, in $[Fe(ptz)_6](BF_4)_2$ the thermal spin transition is accompanied by a crystallographic phase transition. The corresponding thermal transition curves for the super-cooled high-temperature phase as well as the one for the low-temperature phase of $[Fe(ptz)_6](BF_4)_2$ are taken up again in Fig. 9(a). Following the procedure outlined in Section 2, it is straightforward to extract values for Γ and Λ for the low-temperature phase of 144(8) and 380(10) cm^{-1}, respectively [17]. The value for Γ is slightly smaller than the 165(8) cm^{-1} of the high-temperature phase, the one for Λ is slightly larger. In neither of the two phases is Γ large enough to result in a hysteresis on its own. Overall, the thermal transition curve in the low-temperature phase is less abrupt than in the high-temperature phase, and with $T_{1/2}$ extrapolated to 141 K, it is shifted to higher temperatures. Fig. 10(a) shows the HS → LS relaxation curves for the super-cooled high-temperature phase and the low-temperature phase at 52.1 and 40.8 K, respectively. With the above values for Γ and Λ, ΔE°_{HL} ($\gamma_{LS} = 0$) for the latter is slightly larger, and it is therefore not surprising that the initial relaxation in the low-temperature phase is somewhat faster than in the high-temperature phase. However, the much smaller acceleration factor α of only ~ 1, as compared to the value of ~ 5 for the high-temperature phase, is at odds with the value for Γ of 144 cm^{-1}. This apparent discrepancy needs an explanation.

In general, the quantum-mechanical zero-point energy difference between the HS and the LS state, ΔE°_{HL}, in a diluted system is regarded as equal for all complexes in the crystal, and the thermal spin transition is described in terms of a Boltzmann

distribution between the two vibronic manifolds with a fixed value for ΔE°_{HL}. In the mean-field approach to cooperative effects of section two, the zero-point energy difference is assumed to depend upon the specific HS fraction γ_{HS}, but it is still regarded as being equal for all complexes of the crystal for a given value of γ_{HS}. The addition of specific nearest-neighbour interactions in Section 3 modulates ΔE°_{HL} of a given complex according to its immediate surroundings, that is, ΔE°_{HL} of a given complex can take on specific values depending upon the distribution of nearest-neighbour HS and LS complexes.

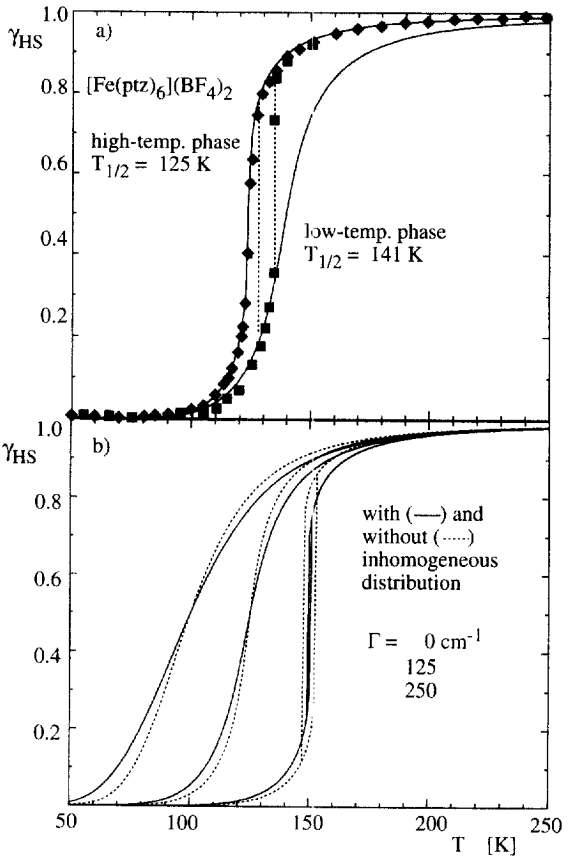

Fig. 9. (a) Thermal spin transition in $[Fe(ptz)_6](BF_4)_2$. High-temperature phase: (◆) experimental, and (—) calculated as for Fig. 1(b), $\Delta H^{\nu\to 0}_{HL} = 462\ cm^{-1}$. $\Delta S^{\nu\to 0}_{HL} = 4.9\ cm^{-1}\ K^{-1}$, $\Lambda = 310\ cm^{-1}$ and $\Gamma = 165\ cm^{-1}$. Low-temperature phase: (■) experimental, and (—) calculated using the same parameters as for the high-T phase except for $\Delta H^{\nu\to 0}_{HL}$ which is taken as a Gaussian distribution with a FWHM of 280 cm^{-1} centred at 520 cm^{-1}. (b) Comparison of transition curves calculated with and without an inhomogeneous distribution of the zero-point energy difference. (i) Non-interacting complexes: (---) $\Delta H^{\nu\to 0}_{HL} = 500\ cm^{-1}$, and (—) Gaussian distribution with FWHM = 200 cm^{-1} around this value, $\Delta S^{\nu\to 0}_{HL} = 5.0\ cm^{-1}\ K^{-1}$. (ii) Interacting system, $\Delta H^{\nu\to 0}_{HL}$ and $\Delta S^{\nu\to 0}_{HL}$ as above, $\Gamma = \Lambda/2 = 125\ cm^{-1}$. (iii) Interacting system with $\Gamma = 250\ cm^{-1}$.

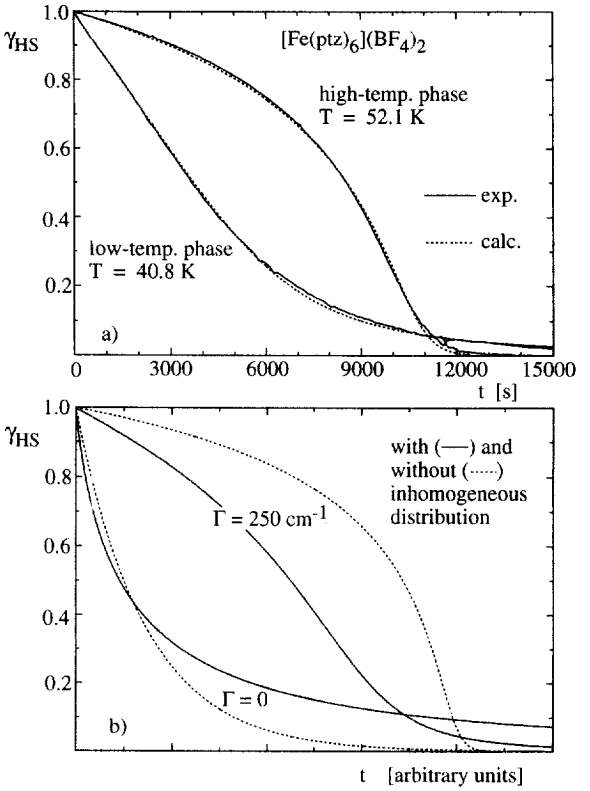

Fig. 10. (a) HS → LS relaxation curves for $[Fe(ptz)_6](BF_4)_2$ in the supercooled high-temperature phase at 52.1 K and in the low-temperature phase at 40.8 K. (—) Experimental; (---) calculated with $S = 45$, $\hbar\omega = 250$ cm^{-1} and $\Gamma = 165$ cm^{-1}. For the high-T phase $n_o = 0.5$, for the low-T phase n_o was taken as a Gaussian distribution with a FWHW = 1.18 (corresponding to ~280 cm^{-1}) around a central value of 1.5. (b) Demonstration of the effect of an inhomogeneous distribution of the zero-point energy difference on the HS → LS relaxation for a system with non-interacting complexes and one with a large interaction. For the calculations $S = 45$, $\hbar\omega = 250$ cm^{-1}, the reduced energy gap $n_o = 1.5$, FWHM of the distribution = 0 and 1 (corresponding to 250 cm^{-1}), and $\Gamma = 0$ and 250 cm^{-1}.

There is another possible source for a modulation of ΔE°_{HL} even for non-interacting complexes in a diluted mixed crystal, namely inhomogeneous broadening [12]. Such broadening is omnipresent. It is usually small, that is < 10 cm^{-1}, for states with small relative displacements along the configurational coordinate and in well crystallised materials, and it may become large, that is > 100 cm^{-1} for states with very large relative displacements and in disordered materials. Of course, such an inhomogeneous distribution would influence both the thermal spin transition as well as the relaxation kinetics. For the thermal spin transition the inhomogeneous distribution of ΔE°_{HL} would manifest itself in a distribution of ΔE°_{HL} around some mean value, whereas ΔS°_{HL}, being basically given by the electronic degeneracies and local vibrational modes, is not affected. Fig. 9(b) shows a comparison of thermal

transition curves calculated according to Eq. (1) for a system of non-interacting complexes, once with a fixed value for $\Delta H^{\circ}_{HL} = 500\ cm^{-1}$ and once with a Gaussian distribution with a full width at half maximum of 200 cm^{-1} centred at 500 cm^{-1}. For both curves ΔS°_{HL} was set to 5 $cm^{-1}\ K^{-1}$. In addition, Fig. 9(b) includes the transition curves calculated according to Eq. (2)), for the same set of parameters but setting $\Gamma = \Delta/2 = 125$ and 250 cm^{-1}. The inhomogeneous distribution tends to flatten the transition curves to some extent, and indeed to reduce the width of the hysteresis, but the overall effect it is not overwhelming.

Fig. 10(b) shows the corresponding HS → LS relaxation curves calculated for the low-temperature tunnelling region. For the system of non-interacting complexes, an inhomogeneous distribution results in deviation from single exponential with a characteristic fast initial decay and a long tail with a much slower decay. This behaviour is, in fact, observable for iron(II) spin-crossover complexes embedded in polymer matrices [30]. For the concentrated system, the effect of an inhomogeneous distribution is to reduce the self-acceleration quite dramatically. Of course for large inhomogeneous distributions the thermal spin transitions, too, will eventually be affected, and indeed, may result in the often observed partial spin transitions [8].

In conclusion, an inhomogeneous distribution, if not too large, does not substantially influence the thermal transition, but it has a dramatic effect upon the low-temperature tunnelling process, because of the exponential dependence of the low-temperature tunnelling rate constant on the zero-point energy difference. With this finding, the apparent discrepancy between the thermal spin transition and the HS → LS relaxation of $[Fe(ptz)_6](BF_4)_2$ in the low-temperature phase can be resolved. The reason for the substantially larger inhomogeneous distribution of the zero-point energy difference between the two states in the low-temperature phase lies in the nature of the phase transition. It is not, as initially proposed, a transition from $R\bar{3}$ to $P\bar{1}$ [31], but it is an order/disorder phase transition within the high-symmetry space group [32], introducing random stacking along the c-axis.

5. Light-induced bistability

For negative values of ΔE°_{HL}, that is with the HS state as the quantum-mechanical ground state of the individual molecules, no thermal spin transition is expected. In such cases it is possible to induce a spin transition by applying an external pressure which stabilises the LS state [33]. In neat materials, ΔE°_{HL} is a function of γ_{LS}. Thus, even if at $\gamma_{LS} = 0$ the HS state is the molecular electronic ground state, an increasing internal pressure with an increasing LS fraction could stabilise the LS state sufficiently to result in it becoming the molecular ground state at $\gamma_{LS} = 1$. In such a case, the LS state would be the thermodynamically stable state of the system at low temperatures. The only problem is, how to get there. The system in the HS state at ambient temperatures has no reason to populate the LS state on lowering the temperature because ΔE°_{HL} at $\gamma_{LS} = 0$ is negative. However, at low temperatures the LS state can in some cases be populated photophysically by irradiating into the spin-allowed d–d absorption band of the HS species. Initially, this LS state is just

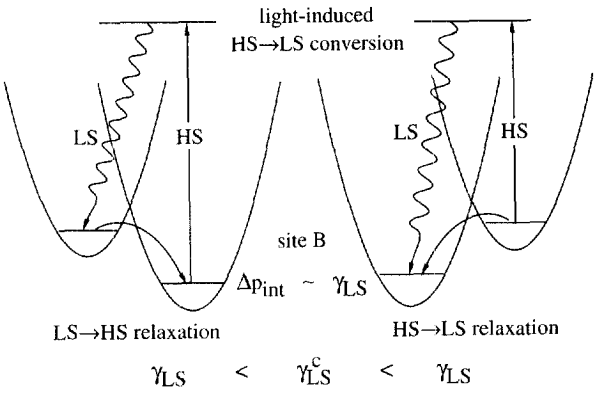

Fig. 11. Schematic illustration of the light-induced bistability for site B in $[Fe(etz)_6](BF_4)_2$.

a metastable state with regard to the individual molecule, but as the light-induced HS → LS conversion proceeds, ΔE°_{HL} may become positive, as schematically shown in Fig. 11.

The $[Fe(etz)_6](BF_4)_2$ spin-crossover compound provides a convincing example of such a light-induced bistability [34]. In this system the iron(II) complexes sit on two non-equivalent lattice sites in a ratio of 2:1. Complexes on one site (denoted as site A) show a comparatively steep thermal spin transition with a transition temperature of 105 K, those on the other site (denoted as site B) stay in the HS state down to liquid helium temperatures, resulting in the transition curve shown in Fig. 12. Complexes on site A behave much like $[Fe(ptz)_6](BF_4)_2$ with regard to light-induced HS ⇄ LS conversions and relaxation processes. Those on site B can be converted almost quantitatively to the LS state at 20 K by irradiating at 820 nm, that is, into the $^5T_2 \rightarrow {}^5E$ band of the HS species. A partial light-induced population of the LS

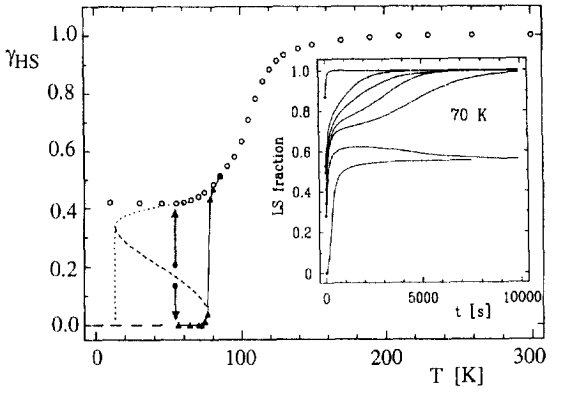

Fig. 12. Thermal spin transition in $[Fe(etz)_6](BF_4)_2$; (○) normal cooling mode; (▲) heating mode after irradiation at 820 nm. Inset: HS → LS relaxation curves following irradiation conditions resulting in different initial overall LS fractions (adapted from Ref. [34]).

state on the two sites results in an interesting relaxation behaviour at temperatures below 80 K (see inset Fig. 12): Complexes on site A always fully relax to the LS state irrespective of the initial LS fraction, because for them ΔE°_{HL} is always positive. For initial values of $\gamma_{LS} < 0.3$, complexes on site B relax to the HS state, and the system ends up with the same overall LS fraction of $\sim 2/3$ as obtained by recording a straightforward transition curve. For initial values of $\gamma_{LS} > 0.3$, however, site B complexes, too, relax to the LS state, so that the system ends up completely in the LS state. At temperatures below 80 K, the cooperative effects thus result in the postulated light-induced bistable behaviour on site B. As the temperature is raised to above 80 K, site B complexes go back to the HS state. This can be regarded as the thermal spin transition in the heating mode of a system with a very large hysteresis. The corresponding branch in cooling mode is not accessible in a simple temperature cycle, because of the macroscopic nature of the energy barrier between the HS and the LS state of the whole crystal.

Very recently, Desaix et al. [35] and Letard et al. [36] reported a light-induced bistability in neat spin-crossover compounds at low temperatures in a steady state type situation under continuous irradiation. This, too, is the direct result of a competition between the light-induced LS→HS conversion and the HS→LS relaxation with the specific dependence of the relaxation rate constant on the LS fraction given by Eq. (7).

6. Conclusions

The aim of this article was not to go into the details of today's sophisticated models of cooperative effects in spin-crossover systems. Rather, we tried to develop a simple, physically meaningful, and, above all, coherent picture of the large variety of observations regarding both the thermal spin transition as well as the HS→LS relaxation.

Microscopically, the individual spin-crossover complexes are regarded as isolated units with well-defined molecular states. Interactions with the surrounding medium basically modulate the zero-point energy difference of the individual complex. In concentrated spin-crossover systems this modulation depends upon the actual state of the whole crystal, due to the elastic forces resulting from the large difference in metal–ligand bond lengths between HS and LS states. The modulation in ΔE°_{HL} can be treated with various degrees of complexity. In mean-field approximation the zero-point energy is assumed to increase linearly with increasing LS fraction, but otherwise it is regarded as identical for all complexes in the crystal at all times. Consequently, HS and LS complexes are always distributed randomly in the crystal for all values of γ_{HS}. This approach works well for highly symmetric systems, for which the reaction coordinate is well described by the totally symmetric breathing mode, such as the model system $[Fe(ptz)_6](BF_4)_2$. In such systems the elastic interactions are of true long-range nature, and the picture of a changing internal pressure is physically meaningful.

In anisotropic systems, for instance with hydrogen bonding between complexes or even bridged systems, specific nearest interactions influence the thermal spin transition and the relaxation behaviour. Such interactions result in non-random distributions of HS and LS complexes. Usually the long-range contribution to the total interaction is still dominant. In these cases nearest neighbour interaction may favour the formation of HS–LS patterns over a certain temperature interval. For $[Fe(pic)_3]Cl_2 \cdot EtOH$, with its step of 7 K in the transition curve, correlation lengths of only a few unit cells were estimated [26,29]. For larger nearest-neighbour interactions, larger steps are observed [37], and super structures may be expected [26].

When interpreting transition curves, in particular with large interaction constants and in crystallographically ill defined systems, for instance in disordered materials, inhomogeneous broadening can lead to false conclusions. It could be one of the reasons for residual HS fractions in a substantial number of spin-crossover compounds [8]. Of course, the width of inhomogeneous distributions very often depends critically upon crystal quality, and thus ill-defined procedures like grinding crystals does influence the transition behaviour [38].

On a molecular scale there is no actual bistability. One state of the system is the ground state, the other can be thermally populated, but the equilibrium is always dynamic. In diluted systems the light-induced high-spin state can only be a metastable state, even at the lowest temperatures, albeit with very long lifetimes due to the small tunnelling probabilities. True bistability, that is infinite lifetime in either of two states, is a phenomenon restricted to the macroscopic world with classical energy barriers, and thus requires cooperative interactions between molecular units, resulting in the well established thermal hysteresis for large values of the interaction constant [4,6]. However, even in spin-crossover systems with very large interactions, the light-induced HS state is never truly stable, because per definition the LS state has to be the molecular ground state at all values of γ_{HS}. The above mentioned bistable behaviour under continuous irradiation [35,36] is not a bistability in a thermodynamic sense either, as it requires a continuous input of non-thermal energy. True light-induced bistability is the result of the special conditions encountered for site B in $[Fe(etz)_6](BF_4)_2$, with the HS state as molecular ground state and the potential for a self-stabilisation of the LS state via a light-induced HS → LS conversion. Of course, in a spin-crossover system with a thermal hysteresis it should, in principle, be possible to induce transitions between the two branches of the transition curve by irradiating the sample with the appropriate wavelength at temperatures within the hysteresis. However, at temperatures above ~ 100 K the HS ⇄ LS relaxation becomes quite rapid, and the light intensities required to disturb the thermal equilibrium by an amount which is large enough to induce the switch, would result in a substantial warming of the sample.

The past few years have indeed seen great advances in the understanding of the various aspects of spin-crossover in iron(II) complexes, not just regarding the thermal spin transition, but also regarding the relaxation kinetics and their photophysical behaviour. Further themes of interest not explicitly covered in this paper include the interplay between the spin transition and crystallographic phase transi-

tions [17,39], the effects of exchange interactions in systems with bridging ligands [40], and the emergence of applications in optical displays which heavily rely on cooperative effects and thermal hysteresis behaviour [13].

Acknowledgements

We thank P. Gütlich, F. Varret and numerous collaborators for their contributions towards the understanding of cooperative effects in spin-crossover compounds. This work was financially supported by the 'Schweizerischer Nationalfonds', the 'Bundesamt für Bildung und Wissenschaft' via a TMR network of the European Union (ERB) (ERB-FMRX-CT98-0199), and the 'Deutsche Forschungsgemeinschaft'.

References

[1] (a) P. Gütlich, Struct. Bond. 44 (1981) 83. (b) E. König, Progr. Inorg. Chem. 35 (1987) 527. (c) J.K. Beattie, Adv. Inorg. Chem. 32 (1988) 1. (d) E. König, Struct. Bonding 76 (1991) 51. (e) P. Gütlich, A. Hauser, H. Spiering, Angew. Chem. Int. Ed. Engl. 33 (1994) 2024.

[2] (a) M.A. Hoselton, L.J. Wilson, R.S. Drago, J. Am. Chem. Soc. 97 (1975) 1722. (b) B.A. Katz, C.E. Strouse, J. Am. Chem. Soc. 101 (1979) 6214. (c) M. Mikami-Kido, Y. Saito, Acta Crystallogr. Sect B 38 (1982) 452. (d) M. Konno, M. Mikami-Kido, Bull. Chem. Soc. Jpn. 64 (1991) 339. (e) J.F. Letard, P. Guinneau, E. Codjovi, G. Bravic, D. Chasseau, O, Kahn, J. Am. Chem. Soc. 119 (1997) 10861.

[3] (a) L. Wiehl, H. Spiering, P. Gütlich, K. Knorr, J. Appl. Cryst. 23 (1990) 151. (b) L. Wiehl, G. Kiel, C.P. Köhler, H. Spiering, P. Gütlich, Inorg. Chem. 25 (1986) 1565. (c) R.A. Binstead, J.K. Beattie, Inorg. Chem. 25 (1986) 1481. (d) P. Adler, A. Hauser, A. Vef, H. Spiering, P. Gütlich, Hyperfine Inter. 47 (1989) 343.

[4] (a) H. Spiering, E. Meissner, H. Köppen, E.W. Müller, P. Gütlich, Chem. Phys. 68 (1982) 65. (b) C.P. Köhler, R. Jakobi, E. Meissner, L. Wiehl, H. Spiering, P. Gütlich, J. Phys. Chem. Solids 51 (1990) 239.

[5] P.L. Franke, J.G. Haasnot, A.P. Zuur, Inorg. Chim. Acta 59 (1982) 5.

[6] (a) J.-P. Martin, J. Zarembowitch, A. Dworkin, J.G. Haasnoot, E. Codjovi, Inorg. Chem. 33 (1994) 2617. (b) J.-P. Martin, J. Zarembowitch, A. Bousseksou, A. Dworkin, J.G. Haasnoot, F. Varret@ Inorg. Chem. 33 (1994) 6325.

[7] H. Köppen, E.W. Müller, C.P. Köhler, H. Spiering, E. Meissner, P. Gütlich, Chem. Phys. Lett. 91 (1982) 348.

[8] (a) P.L. Franke, J.G. Haasnoot, A. Zuur, Inorg. Chim. Acta 59 (1992) 5. (b) K. H. Sugiyarto, K. Weitzner, D.C. Craig, H.A. Goodwin, Aust. J. Chem. 50 (1997) 869. (c) G.A. Renowitch, W.A. Baker, J. Am. Chem. Soc. 89 (1967) 6377.

[9] (a) S. Decurtins, P. Gütlich, K.M. Hasselbach, H. Spiering, A. Hauser, Inorg. Chem. 24 (1985) 2174. (b) A. Hauser, J. Chem. Phys. 94 (1991) 2714.

[10] A. Hauser, Chem. Phys. Lett. 192 (1992) 65.

[11] (a) J. Wajnflasz, J. Phys. Stat. Solidi 40 (1970) 537. (b) C.P. Slichter, H.G. Drickamer, J. Chem. Phys. 56 (1972) 2142.

[12] G.F. Imbusch, R. Kopelman, in: W. Yen, P.M. Selzer (Eds.), Laser Spectroscopy of Solids, Topics in Applied Physics 45, Springer, New York, 1981, p. 1.

[13] (a) O. Kahn, J. Kröber, C. Jay, Adv. Materials, 4 (1992) 718. (b) C. Jay, F. Grolière, O. Kahn, J. Kröber. Mol. Crystallogr. Liq. Crystallogr. 234 (1993) 255. (c) J. Kröber, E. Codjovi, O. Kahn, F.

Grolière, C. Jay, J. Am. Chem. Soc. 115 (1993) 9810. (d) G. Yann, P.J. Van Koningsbruggen, E. Codjovi, R. Lapouyade, O. Kahn, L. Rabardel, J. Mat. Chem. 7 (1997) 857. (e) O. Kahn, C.J. Martinez, Science 279 (1998) 44.

[14] (a) R. Jakobi, H. Spiering, P. Gütlich, J. Phys. Chem. Solids 53 (1992) 267. (b) R. Jakobi, H. Spiering, L. Wiehl, E. Gmelin, P. Gütlich, Inorg. Chem. 27 (1988) 1823. (c) P. Adler, H. Spiering, P. Gütlich, J. Phys. Chem. Solids 48 (1987) 517.

[15] (a) N. Willenbacher, H. Spiering, J. Phys. C Solid State Phys. 21 (1988) 1423. (b) H. Spiering, N. Willenbacher, J. Phys. Condensed Matter 1 (1989) 10089.

[16] J. Jung, G. Schmitt, L. Wiehl, A. Hauser, K. Knorr, H. Spiering, P. Gütlich, Z. Phys. B 100 (1996) 523.

[17] J. Jeftić, A. Hauser, J. Phys. Chem. 101 (1997) 10262.

[18] J.J. McGarvey, I. Lawthers, J. Chem. Soc. Chem. Commun. (1982) 906.

[19] E. Buhks, G. Navon, M. Bixon, J. Jortner, J. Am. Chem. Soc. 102 (1980) 2918.

[20] C.J. Donnelly, G.F. Imbusch, in: B. DiBartolo (Ed.), NATO ASI B245, Plenum Press, New York, 1991, p. 175.

[21] (a) A. Hauser, A. Vef, P. Adler, J. Chem. Phys. 95 (1991) 8710. (b) A. Hauser, Comm. Inorg. Chem. 17 (1995) 17.

[22] C.-L. Xie, D.N. Hendrickson, J. Am. Chem. Soc. 109 (1987) 6981.

[23] K.J. Laidler, Chemical Kinetics, third ed., Harper and Row, New York, 1987, p. 207.

[24] J. Jeftić, R. Hinek, S.C. Capelli, A. Hauser, Inorg. Chem. 36 (1997) 3080

[25] P. Adler, H. Spiering, P. Gütlich, J. Phys. Chem. Solids 50 (1989) 587.

[26] (a) Th. Kohlhaas, H. Spiering, P. Gütlich, Z. Phys. B 102 (1997) 455. (b) H. Spiering et al., this conference.

[27] (a) A. Bousseksou, J. Nasser, J. Linares, K. Boukheddaden, F. Varret, J. Phys I 2 (1992) 1381. (b) A. Bousseksou, F. Varret, J. Nasser, J. Phys I 3 (1992) 1463. (c) H. Bolvin, O. Kahn, Chem. Phys. Lett. 192 (1995) 295.

[28] (a) J. Linares, J. Nasser, K. Boukgeddaden, A. Bousseksou, F. Varret, J. Magn. Mat. 140 (1995) 1507. (b) H. Constant-Machado, J. Linares, F. Varret, J.G. Haasnoot, J.P. Martin, J. Zarembowitch, A. Dworkin, A. Bousseksou, J. Phys. I 6 (1996)1216.

[29] H. Romstedt, A. Hauser, H. Spiering, J. Phys. Chem. Solids 59 (1998) 265.

[30] A. Hauser, J. Adler, P. Gütlich, Chem. Phys. Lett. 152 (1988) 468.

[31] L. Wiehl, Acta Crystallogr. Sect. B 49 (1993) 289.

[32] H. Spiering, J. Kusz, unpublished results.

[33] (a) J.K. McCusker, M. Zvagulis, H.G. Drickamer, D.N. Hendrickson, Inorg. Chem. 28 (1989) 1380. (b) T. Granier, B. Gallois, J. Gauthier, J.-A. Real, J. Zarembowitch, Inorg. Chem. 32 (1993) 5305. (c) E. König, G. Ritter, H. Grünstreudel, J. Dengler, J. Nelson, Inorg. Chem. 33 (1994) 837. (d) C. Roux, J. Zarembowitch, J.-P. Itie, A. Polian, M. Verdaguer, Inorg. Chem. 35 (1996) 574.

[34] (a) R. Hinek, H. Spiering, P. Gütlich, A. Hauser, Chem. Eur. J. 2 (1996) 1435. (b) R. Hinek, H. Spiering, D. Schollmeyer, P. Gütlich, A. Hauser, Chem. Eur. J. 2 (1996) 1427.

[35] A. Desaix, O. Roubeau, J. Jeftic, J.G. Haasnoot, K. Boukheddaden, E. Codjovi, J. Linares, M. Nogues, F. Varret, Eur. Phys. J. B 6 (1998) 183.

[36] J.-F. Letard, P. Guionneau, L. Rabardel, J.A.K. Howard, A.E. Goeta, D. Chasseau, O. Kahn, Inorg. Chem. 37 (1998) 4432.

[37] (a) V. Petrouleas, J.-P. Tuchagues. Chem. Phys. Lett. 137 (1987) 21. (b) J.A. Real, B. Gallois, T. Granier, F. Suez-Panama, J. Zarembowitch, Inorg. Chem. (1992) 4972.

[38] (a) M.S. Haddad, W.D. Federer, M.W. Lynch, D.N. Hendrickson, J. Am. Chem. Soc. 102 (1980) 1468. (b) E.W. Müller, H. Spiering, P. Gütlich, Chem. Phys. Lett. 93 (1982) 567. (c) E.W. Müller, H. Spiering, P. Gütlich, Inorg. Chem. 23 (1984) 119.

[39] (a) Th. Buchen, P. Gütlich, K. H. Sugiyarto, H. A. Goodwin, Chem. Eur. J. 2 (1996) 1134. (b) Th. Buchen, D. Schollmeyer, P. Gütlich, Inorg. Chem. 35 (1996) 155.

[40] A. Real, J. Zarembowitch, O. Kahn, X. Solanes, Inorg. Chem. 26 (1987) 2939.